New Phytologist

Research

Probability distributions of nonstructural carbon ages and transit times provide insights into carbon allocation dynamics of mature trees

David Herrera-Ramírez[1], Jan Muhr[1,2], Henrik Hartmann[1], Christine Römermann[3,4], Susan Trumbore[1] and Carlos A. Sierra[1]

[1]Max Planck Institute for Biogeochemistry, Hans-Knöll-Str 10, Jena 07745, Germany; [2]Department of Bioclimatology, Georg August University Göttingen, Büsgenweg 2, Göttingen 37077, Germany; [3]Institute for Ecology and Evolution, Friedrich Schiller University Jena, Philosophenweg 16, Jena 07743,Germany; [4]German Centre for Integrative Biodiversity Research (iDiv) Halle-Jena-Leipzig, Leipzig D-04103, Germany

Author for correspondence:
David Herrera-Ramirez
Tel: +49 3641 57 6152
Email: dherrera@bgc-jena.mpg.de

Received: *5 November 2019*
Accepted: *16 January 2020*

New Phytologist (2020) **226:** 1299–1311
doi: 10.1111/nph.16461

Key words: carbon ages and transit times, carbon allocation, modeling, nonstructural carbohydrates, tree carbon dynamics, tree storage dynamics.

Summary

In trees, the use of nonstructural carbon (NSC) under limiting conditions impacts the age structure of the NSC pools. We compared model predictions of NSC ages and transit times for *Pinus halepensis*, *Acer rubrum* and *Pinus taeda*, to understand differences in carbon (C) storage dynamics in species with different leaf phenology and growth environments.

We used two C allocation models from the literature to estimate the NSC age and transit time distributions, to simulate C limitation, and to evaluate the sensitivity of the mean ages to changes in allocation fluxes.

Differences in allocation resulted in different NSC age and transit time distributions. The simulated starvation flattened the NSC age distribution and increased the mean NSC transit time, which can be used to estimate the age of the NSC available and the time it would take to exhaust the reserves. Mean NSC ages and transit times were sensitive to C fluxes in roots and allocation of C from wood storage.

Our results demonstrate how trees with different storage traits are expected to react differently to starvation. They also provide a probabilistic explanation for the 'last-in, first-out' pattern of NSC mobilization from well-mixed C pools.

Introduction

The availability and mobility of the nonstructural carbon (NSC) reserves, mostly sugars and starch, determine trees' ability to survive photosynthetic shortages (Dietze *et al.*, 2014; Hartmann & Trumbore, 2016; Martínez-Vilalta *et al.*, 2016; Overdieck, 2016; Trugman *et al.*, 2018; Wiley *et al.*, 2019). Carbon (C) limitation may occur as a result of stresses such as droughts, physical damage, pests, diseases, and floods, which may become more frequent as a result of climatic changes (IPCC, 2018; Klein & Hartmann, 2018). Tree mortality associated with these stressful conditions (Bréda *et al.*, 2006; Carnicer *et al.*, 2011; von Arx *et al.*, 2017) may cause biodiversity loss (Nunez *et al.*, 2019), economic losses (Strand, 2017; Oliveira *et al.*, 2019) and long-term modifications to the global C cycle (McDowell *et al.*, 2018; Pugh *et al.*, 2019). Under stress, trees mobilize NSC from storage to sustain metabolic and growth requirements (Anderegg & Anderegg, 2013; Klein & Hoch, 2015; Mei *et al.*, 2015). Although C allocation has been widely investigated during recent decades, it is a complex process that is still not fully understood (Hartmann & Trumbore, 2016). In general, C fixed during photosynthesis is transported as NSC from chloroplasts to different plant organs (e.g. leaves, branches, stems, and roots) where it is allocated either to metabolism (respiration, growth, defense, osmotic regulation, among others) or to storage, which may occur passively or actively (Lacointe *et al.*, 2004; Wiley *et al.*, 2013; Huang *et al.*, 2019b). To represent and understand these dynamics, compartmental models have been proposed where NSC is allocated to both organ-specific compartments (e.g. leaves, stems and roots) and compound-specific compartments (Richardson *et al.*, 2012; Klein & Hoch, 2015; Ceballos-Núñez *et al.*, 2018).

One example of recent advances is the observation that the ^{14}C-modeled mean age of NSC in tree stems increases with depth in the stem. This has been modeled in two ways. Richardson *et al.* (2015) proposed a two-pool model of NSC with: 'active' (< 1 yr old) labile C that is quickly cycled through the tree and replenished mostly by the influx of newly assimilated C; and 'stored', older NSC that accumulates when photosynthesis surpasses demand and is retrieved at slow rates. These two compartments have been associated with specific compounds – sugar and starch – (Klein & Hoch, 2015). However, the similar ages reported for sugar and starch pools using ^{14}C do not support this

generalization (Richardson *et al.*, 2015). Despite recent efforts, it is still difficult to differentiate and measure fast and slow cycling pools of NSC in trees. Alternatively, Trumbore *et al.* (2015) explained the increasing ages of NSC with depth in stem-wood using a simple diffusion model of one NSC compartment and radial mixing of mobile C of different ages. In this model, the net mixture of NSC inwards from the phloem along rays is a source of NSC that is younger than the structural C where it is found. The ability of different models to explain the same observation indicates the importance of a model representation of C allocation for improving our ability to estimate and understand NSC dynamics.

In trees, NSC dynamics determine the age and transit time distributions of the C in the different organ-specific and compound-specific pools (Ceballos-Núñez *et al.*, 2018). Carbon age is defined as the time elapsed after a C atom enters the system until the time of observation (Bolin & Rodhe, 1973), that is, an age of zero represents the moment of C fixation from the atmosphere. Transit time is defined as the time that a C atom remains in the system until it exits (Ceballos-Núñez *et al.*, 2018). To give an example: when defining our observed system as all the NSC in a tree, C atoms would enter through photosynthesis (with age equal to zero) and leave when being allocated to the formation of structural tissue (growth) or to catabolic requirements (e.g. loss as CO_2). Here, we define NSC transit time as the time elapsed between these two points. These definitions allow us to estimate the distributions of the NSC ages and NSC transit times across all C pools using models (Ceballos-Núñez *et al.*, 2018; Metzler *et al.*, 2018). This offers a useful alternative to evaluate NSC dynamics in trees. While the precise measurement of these quantities remains elusive, the mean age and mean transit time of the NSC of different organs have been estimated from ^{14}C measurements in the sugars and the respired $^{14}CO_2$, respectively, and by pulse-labeling techniques in trees (Carbone *et al.*, 2006, 2013; Epron *et al.*, 2012; Trumbore *et al.*, 2015; Muhr *et al.*, 2016, 2018).

For healthy, unstressed trees not experiencing C limitation, NSC in respiration and growth consists mainly of C from the current growth year (< 1 yr old) (Richardson *et al.*, 2015; Muhr *et al.*, 2018). However, previous studies have shown that trees under C supply limitation start mobilizing stored C, resulting in an increase in the mean age of the C used for new growth or metabolism (Vargas *et al.*, 2009; Carbone *et al.*, 2013; Trumbore *et al.*, 2015; Ceballos-Núñez *et al.*, 2018; Muhr *et al.*, 2018). How the quantity and mobility of stored C vary with tree species and/or between organs in the same tree will result in different age and transit time distributions. To date, we lack a systematic understanding about how NSC age distributions differ between tree organs and tree species, and about the differences in the use of the NSC reserves under outstanding C limitation. To answer these questions and to test hypotheses about C allocation strategies in trees, it is important to have the ability to estimate NSC age and transit time distributions.

The representation of C allocation in compartmental systems allows such estimation of NSC age and transit time distributions (Ceballos-Núñez *et al.*, 2018; Metzler *et al.*, 2018; Metzler & Sierra, 2018). These distributions describe the relative abundance of C of different ages in each NSC pool. By compartmentalizing two whole-tree C allocation models proposed by Klein & Hoch (2015) and Ogle & Pacala (2009), and estimating the age and transit time distributions based on the mathematical framework developed by Metzler & Sierra (2018) and Metzler *et al.* (2018), we address here three main questions: (1) how different are the predictions of NSC dynamics overall and between tree organs, for contrasting plant types (evergreen vs deciduous) or for contrasting environmental conditions (severe growth limitations vs. favorable conditions)? (2) what is the predicted age structure of the NSC reserves available and how long, theoretically, trees would take to consume these reserves? and (3) what are the principal C fluxes that influence the NSC mean ages and mean transit times? We expect that compartmental models, which consider organ-specific and compound-specific C pools, will allow us to estimate differences in the NSC age distributions of trees with different life strategies, and to associate them with different storage traits. We also expect that, by estimating the changes of the NSC transit time during severe C limitation, we can describe the age structure of the C available for sustaining the tree's metabolism and growth and to estimate how long it can take for the trees to exhaust their reserves.

Materials and Methods

Model descriptions

We used compartmental linear models of C allocation in individual trees to estimate NSC age and transit time distributions (Figs 1, 2). We used species of different leaf phenology – evergreen and deciduous – and different growth environments, Mediterranean and temperate forest. Compartmental models describe the exchange of mass between compartments following mass conservation principles (Jacquez & Simon, 1993; Metzler & Sierra, 2018). This means that the mass of NSC leaving each compartment is a fraction of the mass of the NSC compartment, and the mass entering the compartment is immediately mixed with the mass of the NSC compartment, making the mass of the compartment homogeneous at any time (Metzler & Sierra, 2018). The structures of the compartmental linear models follow those described in Klein & Hoch (2015) for *Pinus halepensis* Mill. and in Ogle & Pacala (2009) for *Acer rubrum* L. and *Pinus taeda* L. with small variations based on theoretical assumptions (Figs 1, 2). We estimated the model parameters (annual fraction of C transferred between pools) based on the C fluxes and pool stocks reported in the two studies for each species (Tables 1, 2).

The model proposed by Klein & Hoch (2015) was parameterized using a C balance approach and exhaustive ecophysiological measurements during more than 13 yr at Yatir forest, Israel. *Pinus halepensis* occurs in humid Mediterranean regions, but Yatir forest is a semiarid forest with only 285 mm of annual precipitation and an extended drought period of several months, so trees there are at the limit of the species' growth requirements (Klein & Hoch, 2015). Model parameters were estimated for a typical mature and healthy tree where the amount of C fixed was

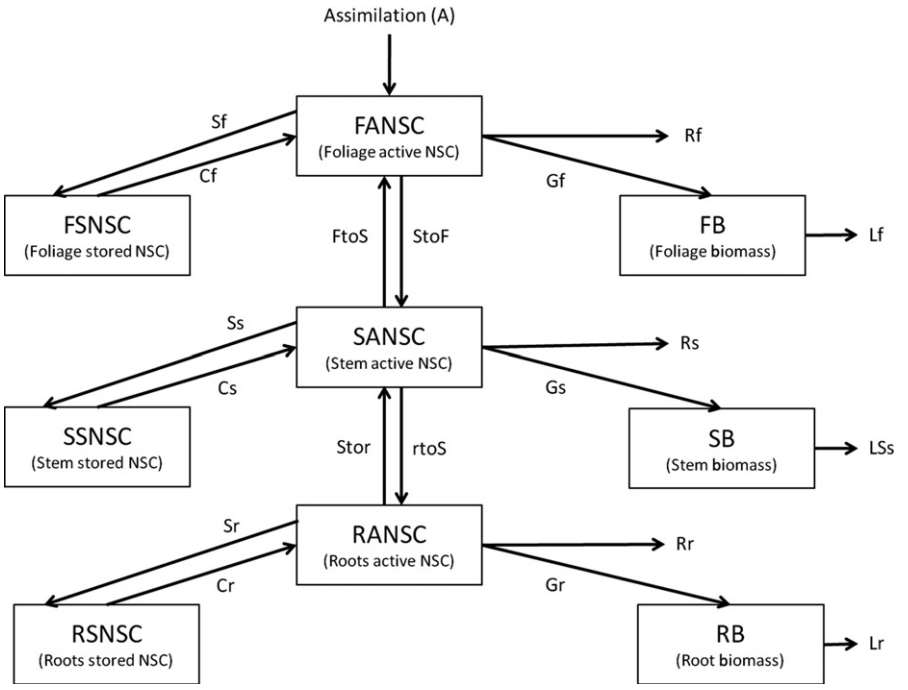

Fig. 1 Compartmental representation of the carbon allocation model proposed for the evergreen Mediterranean *Pinus halepensis* by Klein & Hoch (2015). The square compartments define the state variables, and the arrows define the fraction of carbon that is transferred between pools. The name and values of the transfer coefficients and state variables are defined in Tables 1 and 2. This model is described by the Eqn 1.

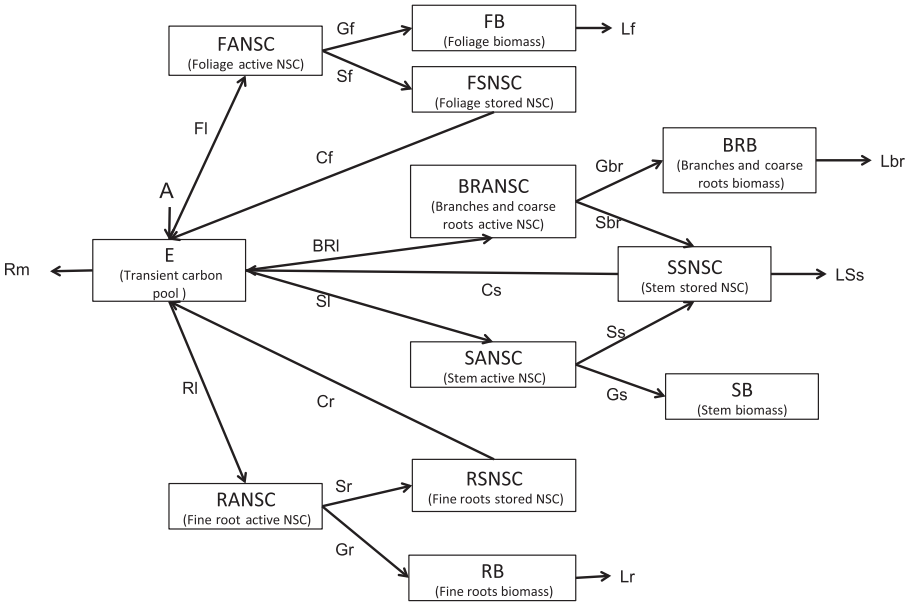

Fig. 2 Compartmental representation of the carbon allocation model proposed for the temperate deciduous *Acer rubrum* and evergreen *Pinus taeda* species based on a theoretical interpretation of the 'Allometrically constrained growth and C allocation' model (ACGCA) developed by Ogle & Pacala (2009). The square compartments define the state variables, and the arrows define the fraction of carbon that is transferred between pools. The name of the transfer coefficients and state variables are defined in Tables 1 and 2. This model is described by the Eqn 1.

assumed to be very close to the amount of C released, that is, trees were close to a steady-state condition with respect to C (Klein & Hoch, 2015). Three organ-specific C pools were defined as stem, foliage and below ground, each with three compound-specific C pools: starch (stored NSC), soluble sugars (active NSC) and structural carbohydrates (i.e. biomass) (Fig. 1). In the original model, the starch and soluble sugars were categorized into stored (slow cycling) and active (fast cycling) NSC pools, respectively. All fluxes of C were reported in the original publication in g C d^{-1} per tree and converted to g C yr^{-1}. Then, we calculated the annual fraction of C that leaves each pool (yr^{-1}), that is, the ratio of flux divided by pool size of the donor pool. These fractions were used as the parameters for the model (Fig. 1; Table 2).

Ogle & Pacala (2009) proposed a mechanistic model named 'Allometrically constrained growth and C allocation' (ACGCA). We used the ACGCA model to estimate the fluxes and pool sizes of the model in Fig. 2 for a typical mature and healthy tree of both species *A. rubrum* and *P. taeda* at steady state (Table 2). The parameters for steady state were obtained after running the ACGCA model for 700 time steps, to the point where pool sizes and fluxes did not change with time. ACGCA estimates the pool stocks in grams of glucose per tree (g Gluc) and the fluxes in grams of glucose per tree $year^{-1}$ (g Gluc yr^{-1}). Here, we converted

Table 1 Compartment names of the models described in Figs 1 and 2.

Abbreviation	Name
E	Transient carbon pool
FANSC	Foliage active nonstructural carbon
FSNSC	Foliage stored nonstructural carbon
FB	Foliage biomass
BRANSC	Branches and coarse roots active nonstructural carbon
BRB	Branches and coarse roots biomass
SANSC	Stem active nonstructural carbon
SB	Stem biomass
SSNSC	Stem stored nonstructural carbon
RANSC	Fine roots active nonstructural carbon
RSNSC	Fine roots stored nonstructural carbon
RB	Fine root biomass

these parameter values to g C and g C yr^{-1}, respectively, based on the molar masses of C and glucose (12 and 180.15 g mol^{-1}, respectively). Then, the model parameters were also calculated by dividing the flux value by the size of the compartment from which C was removed, obtaining the annual fraction of C leaving each pool.

The ACGCA model was designed to estimate growth and reproduce a range of physiological states defined by tree's allometries and labile C (NSC) status (Ogle & Pacala, 2009). The model we used for our estimations and simulations follows a linear compartmental interpretation of the ACGCA model. This model is structurally similar to the one used for *P. halepensis*: it considers organ-specific C pools as foliage, branches and coarse roots, stem, and fine roots; and compound-specific C pools as transient NSC, active NSC, stored NSC, and structural carbohydrates per tree organ (Fig. 2). Nevertheless, the chemical nature of the C in these pools is restricted to glucose; no differentiation between starch and sugar is made.

These models were described with a system of ordinary differential equations expressed in the general linear nonautonomous form presented in Ceballos-Núñez *et al.,* (2018):

$$\frac{dx(t)}{dt} = B \cdot x(t) + b \cdot u(t), x(t=0) = x_0, \quad \text{Eqn 1}$$

where $\frac{dx(t)}{dt}$ is the vector of rates of change of C with respect to time in each compartment; **B** is a $m \times m$ square matrix, where m is the number of compartments in the model, the diagonal

Table 2 Annual mean and standard deviation (SD) of the carbon transfer coefficients (yr^{-1}) for the models in Figs 1 and 2 for the species *Pinus halepensis* (model from Klein & Hoch, 2015), *Acer rubrum* and *Pinus taeda* ('Allometrically constrained growth and C allocation' model (ACGCA) from Ogle & Pacala, 2009).

		P. halepensis		*A. rubrum*		*P. taeda*	
Abbreviations	Parameter Name	Mean	SD	Mean	SD	Mean	SD
A	Assimilation at steady state	23 520		211 770		200 090	
Rm	Maintenance respiration			0.25	0.053	0.167	0.033
Fl	Allocation to FANSC			0.05	0.004	0.042	0.011
BRl	Allocation to BRANSC			0.669	0.054	0.757	0.044
Sl	Allocation to SANSC			1.00E-04	3.00E-03	6.24E-06	0.004
Rl	Allocation to RANSC			0.031	0.006	0.035	0.016
Rf	Respiration foliage	9.56	0.72				
Rbr	Respiration branches and roots						
Rs	Respiration stem	0.59	0.026				
Rr	Respiration roots	16.84	0.23				
Gf	Growth foliage	2.94	0.05	0.939	0.003	0.932	0.015
Gbr	Growth branches and coarse roots			0.912	0.001	0.943	0.007
Gs	Growth stem	0.3	0.02	0.912	0.001	0.943	0.007
Gr	Growth roots	1.28	0.21	0.893	0.026	0.942	0.019
Lf	Litterfall foliage	0.34	0.07	1	0	0.333	0.089
Lbr	Litterfall branches and roots			0.047	0.021	0.047	0.018
Lr	Literfall fine roots	0.07	0.01	1	0.055	0.5	0.21
LSs	Stored NSC lost in wood conversion to heartwood and litter fall	0.003	0.0005	0.031	0.007	0.06	0.006
Sf	Allocation to storage in foliage (FSNSC)	0.44	0.4	0.061	0.003	0.068	0.015
Sbr	Allocation to storage in wood of branches and coarse roots (SSNSC)			0.088	0.001	0.057	0.007
Ss	Allocation to storage in stem (SSNSC)	0.8	0.05	0.088	0.001	0.057	0.007
Sr	Allocation to storage in roots (RSNSC)	4.98	2.64	0.107	0.026	0.058	0.019
Cf	Allocation from storage in foliage (FSNSC) to E	2.02	0.68	1	0	0.333	0.089
Cs	Allocation from storage in stem (SSNSC) to E	1.09	0.7	0.023	0.01	0.023	0.009
Cr	Allocation from storage in roots (RSNSC) to E	1.22	0.58	1	0.055	0.5	0.21
FtoS	Allocation from foliage to stem	33.7	3.2				
StoF	Allocation from stem to foliage	0.04	0.043				
Stor	Allocation from stem to roots	3.15	0.86				
rtoS	Allocation from roots to stem	0.11	0.11				

Pool name abbreviations are defined in Table 1.

elements of the matrix are the fraction of C leaving each pool and the off-diagonal entries represent the fraction of C transferred among compartments; $x(t)$ is the vector of mass of C in each compartment; b is the vector of partitioning of the photosynthetic input $u(t)$; and x_0 is a vector of initial values of the C compartments.

Estimation of NSC ages and transit times of mature and healthy trees (close to steady state)

The description of the models in the system of differential equations (Eqn 1) allowed us to estimate the age and transit time distributions at steady state for each species. Here, we interpret steady state as the condition of mature and healthy trees whose C uptake is nearly balanced by respiration and litter fall. These distributions were calculated as the sum of exponential distributions using the formulas developed by Metzler & Sierra (2018). The age density distribution of the C that is in the system is given by the probability of finding C particles of a certain age $y \geq 0 (f_A(y))$ and it follows the equation.

$$f_A(y) = z^T \cdot e^{y \cdot B} \cdot \frac{x^*}{||x^*||}, y \geq 0, \quad \text{Eqn 2}$$

where z^T is the vector of release rates from the system, e^{yB} is the matrix exponential evaluated at age y, and interpreted as the probability matrix of transfers among compartments, $\frac{x^*}{||x^*||}$ is the distribution of C among the different pools, and x^* is the steady-state content of the system (Eqn 1). We use here the symbol $||\cdot||$ to represent the vector norm, which is the sum of the absolute values of all entries of the vector.

The mean age is given by the expected value ($E[A]$).

$$E[A] = \frac{||B^{-1} \cdot x^*||}{||x^*||}. \quad \text{Eqn 3}$$

Transit time can be considered as forward transit time (FFT) or backward transit time (BTT) (Metzler *et al.*, 2018). The FFT is the time a particle would take to travel the system after its arrival at a given time. The BTT is the age that a particle has when it leaves the system. Therefore, the BTT density distribution ($f_{BTT}(y)$) describes the probability that a C particle has a certain age y when it leaves the system at time t. As our aim concerns the age of the C when it leaves the system, we will deal here with the BTT only expressed as:

$$f_{BTT}(y) = z^T \cdot e^{y \cdot B} \cdot \beta, y \geq 0. \quad \text{Eqn 4}$$

The mean backward transit time is defined as ($E[\mathrm{BTT}]$):

$$E[BTT] = \frac{||x^*||}{||u||}. \quad \text{Eqn 5}$$

Note that the definitions presented here can only be applied to autonomous systems at steady state (Metzler & Sierra, 2018). Therefore, these formulas were used to characterize the NSC dynamics of mature and healthy trees where the C inflow u and the coefficients in $\boldsymbol{B}$ do not change over time. To characterize NSC dynamics, the age and transit time distributions were calculated only for the NSC pools of the described models in Figs 1 and 2.

Estimation of NSC ages and transit times of trees under C source limitation (out of steady state)

We estimated time-dependent NSC age and transit time distributions for 40 yr after the assimilation input ($u(t)$) was set to zero ($f_A(y,t), f_{BTT}(y,t)$), while keeping the transfer C coefficients (matrix $\boldsymbol{B}$) constant. We used zero assimilation to have a clear view of how trees use their NSC when they depend exclusively on storage. This approach allowed us to evaluate how limitations in C assimilation would impact the age and transit time distributions of C in mature and healthy trees. The changes in these quantities reflect the age of remaining NSC reserves and the age of C used for respiration at each time step under C limitation.

In our simulations, we kept the assimilation flux $u(t)$ constant at the values reported for healthy trees in steady state (Table 2) for the first 10 yr ($t < t_0$), and then set it to zero in any subsequent time $t \geq t_0$ until $t = 50$. Until t_0, the NSC age and transit time distributions $f_A(y)$ and $f_{BTT}(y)$ did not change. These distributions constitute the initial (steady state) conditions for the system before the C limitation. The mathematical framework for estimating the age and transit time distributions when the elements of the system (Eqn 1) depend on time, and are out of steady state, was developed by Metzler *et al.*, (2018). The approach consists of solving the system of differential equations (Eqn 1) first, and then taking this solution to reconstruct an analogous linear system of differential equations with the same solution trajectory. From the new system, it is possible to obtain a mathematical object called the state transition operator, which encapsulates all the dynamics of the system, including the probabilities of C particles moving from one pool to another. As we know the initial age distributions from the steady-state system, we use the state transition operator to move the initial age distribution forward in time. We therefore estimated the NSC age and transit time distributions and their respective mean values for the subsequent times $t > t_0$. We calculated the percentage of the NSC consumed in each time step after the C limitation started by computing the solutions of each model (Eqn 1) for each time step, which gives us the amount of the NSC remaining in each C pool, and then subtracting this quantity from the initial amount of NSC in the system. We used the Python packages 'BGC-MD' and 'CompartmentalSystems', which implement the formulas required for these computations (Metzler *et al.*, 2018).

Sensitivity and uncertainty of the NSC mean age and mean transit time to variations in sink strength

To understand the sensitivity of the NSC mean age and mean transit time at steady state to changes in the sink C fluxes, we evaluated the change in NSC mean age and mean transit time to a given numerical alteration of the fraction of C leaving each pool

(coefficients of matrix $\boldsymbol{B}$ in Eqn 1). This analysis allowed us to identify the pool-specific fluxes that have the greatest influence on the overall NSC ages and transit times in mature trees. For that, we used the method 'Elementary effects' (Morris, 1991; Campolongo *et al.*, 2007). This method analyzes the change in model output if exactly one parameter (p_i) is changed by a random fraction (dp_i) between L levels (150) in the parameter space. The parameter space was estimated based on the parameter variability provided by Klein & Hoch (2015) and Ogle & Pacala (2009) (Table 2). It then changes each parameter once and repeats this process throughout p (parameters) + 1 simulations which are called a 'trajectory' (Cuntz *et al.*, 2015). We then ran 100 trajectories. We estimated a bigger parameter space than the one reported for each species to capture a more general trend outside of the limits of each species. Then, the elementary effect of each parameter EE_i in each trajectory is calculated as a differential quotient:

$$EE_i = \frac{f(p_i + dp_i) - f(p_i)}{\delta}, \qquad \text{Eqn 6}$$

where δ is dp_i as a fraction of the dp_i range. The mean μ^* and the variance σ of the absolute values of the EE_i from the 100 trajectories were used as a measure of sensitivity (Cuntz *et al.*, 2015). The elementary effects simulations and calculations were done using the R packages SENSITIVITY v.1.15.2 (Iooss *et al.*, 2019) and SOILR (Sierra *et al.*, 2014).

To evaluate how the uncertainty in the models' parameters affects the mean age and the mean transit time of the species evaluated, a Monte Carlo Simulation (MCS) analysis was performed. This method involves repeated model realizations of a random selection of parameter values (Parkinson & Young, 1998). The standard deviation associated with each parameter has been derived from Klein & Hoch (2015) for *P. halepensis* and from Ogle & Pacala (2009) for *A. rubrum* and *P. taeda* (Table 2). Then we ran 1000 MCSs to estimate the corresponding standard deviation of the mean age and mean transit time of the NSC for the whole tree and for each C pool. Only the most influential parameters of each model were resampled assuming they come from independent Gaussian distributions. This assumption of independence is potentially limiting, given that the MCS analysis would yield different results if there were covariance between the parameters. However, the degree of association between parameters is unknown to us. If better information on their correlation were available, this uncertainty could be re-estimated.

Data deposition

The R and PYTHON code used to generate all the data reported in this article are provided in the following repository: https://github.com/MPIBGC-TEE/Probability_distributions_of_NSC_ages_and_transit_times

Results

NSC ages and transit times of mature and healthy trees (trees close to steady state)

Different tree species of contrasting functional types had distinct NSC age and transit time distributions (Figs 3, 5). For simplicity, we use the mean values of these distributions to describe these differences here. For *P. halepensis,* the mean NSC transit time –

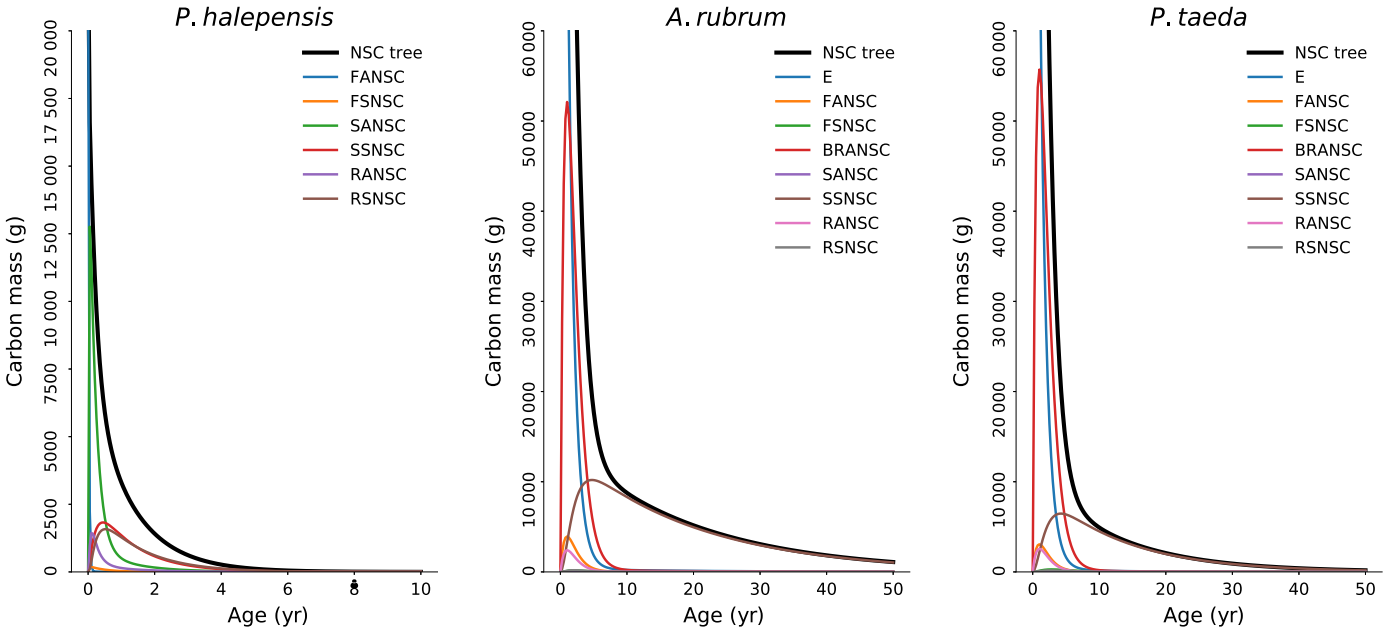

Fig. 3 Age distributions of the nonstructural carbon in the whole tree and tree pools for each species *Pinus halepensis*, *Acer rubrum* and *Pinus taeda*. The frequencies are given in grams of carbon and the sum of all the frequencies of all the compartments is equal to the total mass of carbon of the system. The acronyms in the key in each panel are defined in Table 1.

Table 3 Mean age ± standard deviation for the different carbon pools in *Pinus halepensis*, *Acer rubrum* and *Pinus taeda* (in yr).

Pool name	*P. halepensis*	*A. rubrum*	*P. taeda*
NSC tree	0.98 ± 0.38	9.45 ± 3.7	4.4 ± 0.72
E		1.55 ± 0.20	1.19 ± 0.06
FANSC	0.03 ± 0.001	2.55 ± 0.20	2.19 ± 0.06
FSNSC	0.52 ± 0.001	3.56 ± 0.20	5.22 ± 0.06
SANSC	0.045 ± 0.10	2.55 ± 0.20	2.19 ± 0.06
SSNSC	1.370 ± 0.58	21.3 ± 5.38	14.22 ± 1.63
RANSC	0.730 ± 0.76	2.55 ± 0.20	2.19 ± 0.06
RSNSC	1.550 ± 0.12	3.55 ± 0.20	4.19 ± 0.06

Pool name abbreviations are defined in Table 1.

Table 4 Mean age ± standard deviation for the different organ-specific pools in *Pinus halepensis*, *Acer rubrum* and *Pinus taeda* (in yr).

Organ	*P. halepensis*	*A. rubrum*	*P. taeda*
Leaves	0.07 ± 0.001	1.98 ± 0.20	1.91 ± 0.06
Stem	0.73 ± 0.580	9.97 ± 5.38	4.58 ± 1.63
Roots	1.33 ± 0.760	2.01 ± 0.20	2.36 ± 0.06

the age of C being used in metabolism and growth – was very young (0.49 ± 0.08 yr). Likewise, the overall mean NSC age – the age of the C remaining in the tree – was also very young (0.98 ± 0.38 yr). By contrast, the temperate species *A. rubrum* and *P. taeda* had slower predicted C cycling with mean ages of 9.45 ± 3.7 and 4.4 ± 0.72 yr and transit times of 2.95 ± 0.31 and 2.4 ± 0.09 yr, respectively.

The predicted NSC age and transit time distributions among different C pools showed contrasting behaviors. NSC age distributions for all the NSC pools in *P. halepensis* were similar across tissues (Fig. 3; Table 3). For this species, the NSC stored in stem and roots had the oldest mean ages (Table 3). By contrast, there was a clear distinction in the predicted mean ages of active and stored NSC pools for the temperate species *A. rubrum* and *P. taeda* (Table 3). The NSC stored in the stem had a mean age of 21.3 ± 5.38 yr in *A. rubrum*, but only 14.2 ± 1.63 yr in *P. taeda*. The mean ages of NSC stored in the foliage and fine roots (FSNSC and RSNSC pools) were lower in *A. rubrum* (3.5 ± 0.20 and 2.5 ± 0.20 yr respectively) than in *P. taeda* (5.2 ± 0.06 and 4.19 ± 0.06 yr, respectively; Table 3). In general, the age of the NSC in leaves was greater than we expected, especially in the deciduous tree *A. rubrum*. Overall, the age of the NSC in each tree organ is given by the combination of the NSC ages of the compound-specific compartments – active, stored and transient NSC pools – in each respective organ. Mean age estimates of the NSC in leaves and fine roots are < 2 yr (Table 4). In the stem, mean ages of NSC were 0.73 ± 0.58, 9.97 ± 5.38 and 4.58 ± 1.63 yr for *P. halepensis*, *A. rubrum* and *P. taeda* respectively (Table 4).

Nonstructural C age and transit time distributions characterized in detail the age composition of the NSC that remains in and leaves the tree (Figs 3, 5). The mixture of NSC ages for mature healthy trees followed a phase type distribution (Fig. 3), which is a mixture of exponential distributions (Metzler & Sierra, 2018). The shape of the distributions depended on the speed at which the C was cycled within the tree. Carbon age distributions allowed us to better understand the age composition of each C pool. For instance, for *P. halepensis*, 95% of all NSC in the entire tree was younger than 3.3 yr. For *A. rubrum*, 95% of the NSC was < 42 yr old, and NSC respired or allocated to growth did not exceed 2.9 yr. In *P. taeda*, 95% of all NSC was < 20 yr old, while 95% of the NSC leaving the system was younger than 2.4 yr old. The trees' NSC pools had different NSC age and transit time compositions (Figs 3, 5), which characterize the different dynamics of each NSC compartment in the trees' C balance.

NSC ages and transit times of trees under carbon source limitation (out of steady state)

When simulating C limitation for the trees characterized in Fig. 3, our model predicted changes in the shape of the NSC age and transit time distributions over time as a result of NSC storage mobilization (Figs 4, 5). The simulated C limitation progressively reduced the mass of NSC in storage compartments (Fig. 4). The C mass drawn from storage was younger during the initial phase of the simulations and increased during the simulations (Fig. 5). The proportion of young C decreased rapidly, flattening the entire NSC age distribution of the trees (Fig. 4). Consequently, both the mean age and mean transit time of the NSC increased as C limitation progressed. The mean transit time increased first in an exponential way and then linearly (Fig. 6). The exponential phase reflects the progressive and fast depletion of young reserves and increasing importance but slower utilization of old C. Then, when the age distribution of the remaining NSC becomes increasingly uniform, the linear phase describes the aging of the remaining C.

The increase in mean transit time during C limitation indicates that trees used increasingly older reserves for respiration as the storage pool was exhausted. For trees that can store C for a longer time, such as *A. rubrum* and *P. taeda*, the cessation of assimilation resulted in an increase in the mean transit time of several years, principally as a result of the availability of several decades old NSC in the stem and coarse roots to support metabolism (Fig. 3). For *A. rubrum*, the mean transit time increased from 2.9 ± 0.31 yr in healthy conditions to 10.3 ± 0.31 yr when trees had consumed 50–60% of the reserves, and to 21 ± 0.31 yr when only 20% of their reserves remained (Fig. 6). For *P. taeda*, mean transit times increased from 2.4 ± 0.09 yr at steady state to 5 ± 0.09 yr (50–60% consumption), and to 13 ± 0.09 yr (80% consumed) (Fig. 6). For *P. halepensis* trees growing in Yatir forest, the transit time increased from 0.48 ± 0.08 to 4 ± 0.08 yr at the end of the exponential trend (Fig. 6).

Sensitivity and uncertainty of mean age and mean transit time to variations in sink strength

The mean age was mainly sensitive to changes in the consumption of NSC from stored C in the stem, branches and coarse roots (Cs) and the loss of NSC in the transition from sapwood to

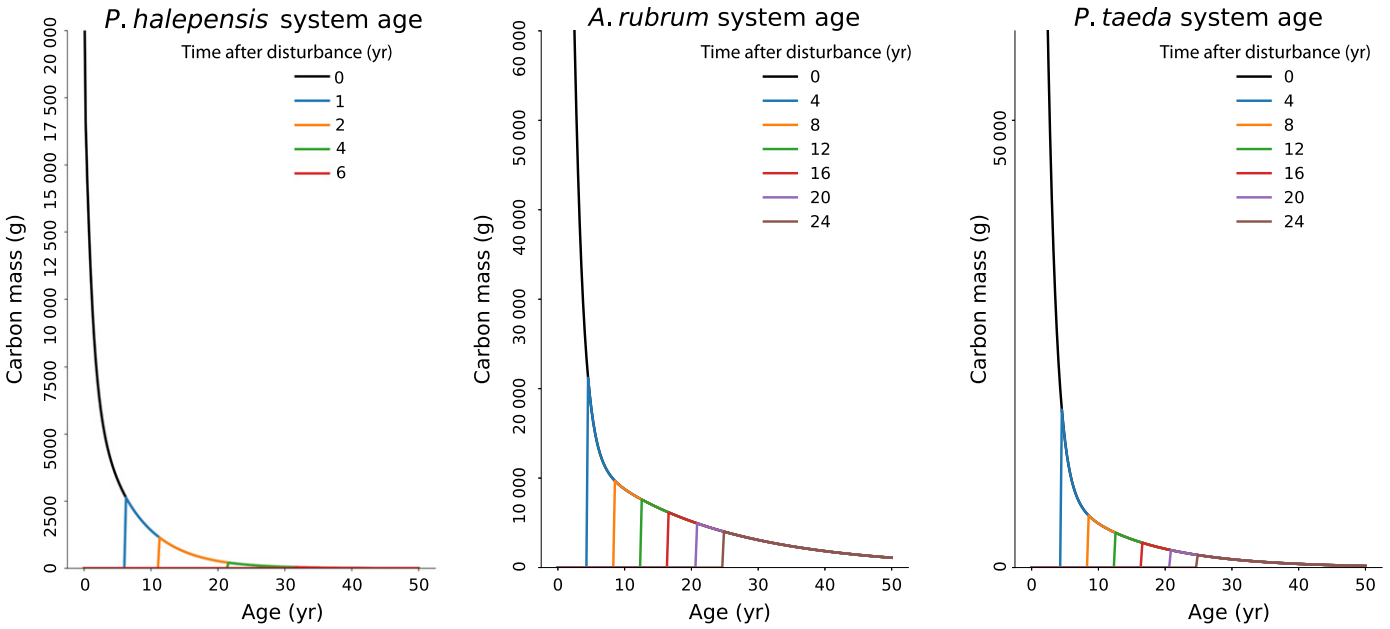

Fig. 4 Age distribution of the nonstructural carbon in the whole tree for years subsequent to the start of the carbon limitation simulation (yr after disturbance) for each of the species *Pinus halepensis*, *Acer rubrum* and *Pinus taeda*.

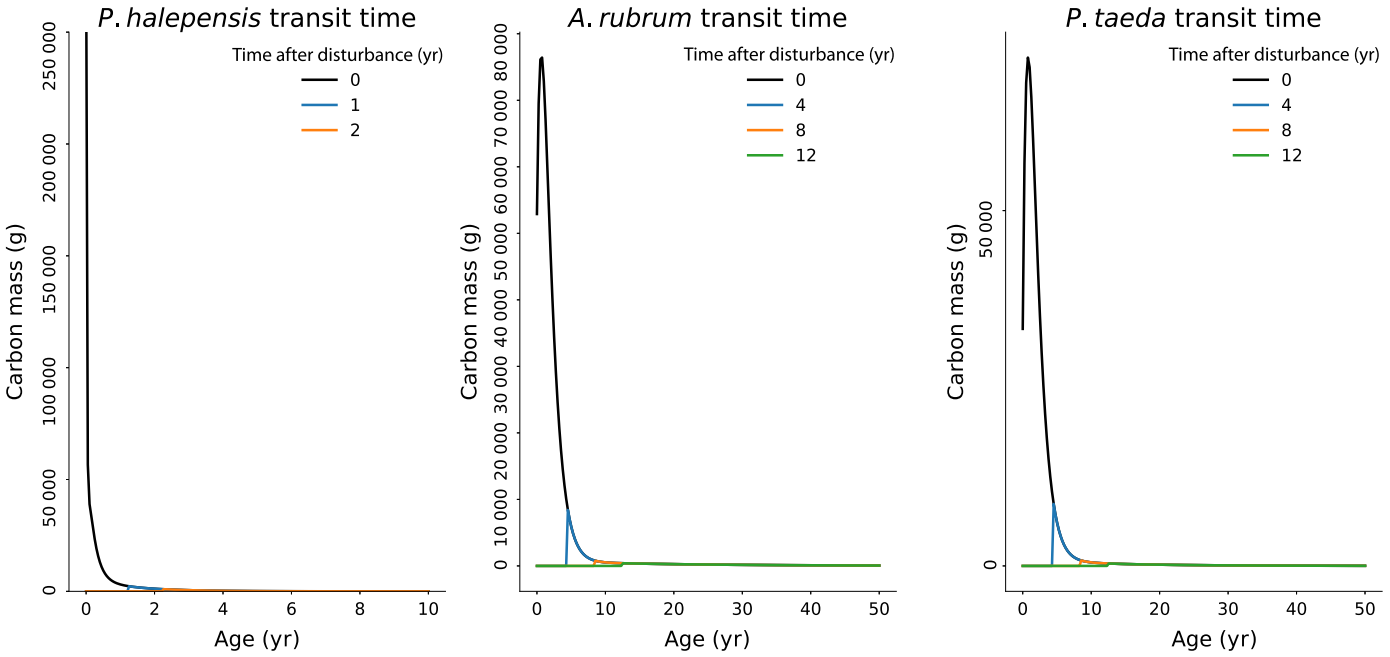

Fig. 5 Backward transit time distributions of the nonstructural carbon in the whole tree for years before the carbon limitation (year 0 after disturbance) and years subsequent to the start of the simulated carbon limitation for each of the species *Pinus halepensis*, *Acer rubrum* and *Pinus taeda*.

heartwood (LSs) (Supporting Information Fig. S1). The mean transit time was principally sensitive to the allocation of NSC to storage in the roots (Sr and Sbr) and root growth (Gr). In addition, both quantities were sensitive to changes in the allocation to root active NSC (Stor and BRl) and, to a lesser degree, to root respiration (Rr) (Fig. S1). The impact of changes in these cycling rates on the mean age and mean transit time is complex and nonlinear in some cases, as indicated by high variance of the sensitivity index (Figs S1, S2). But in general, the higher the consumption from the NSC stem pools, the younger the NSC in the tree; and the greater the storage of NSC in the roots, the older the NSC in the tree.

The mean uncertainty (1.5 yr) in the mean ages and transit times reflected uncertainties in the most influential cycling rates, as described earlier. This uncertainty was smaller than the mean differences between species (5.97 yr). In general, *A. rubrum* had

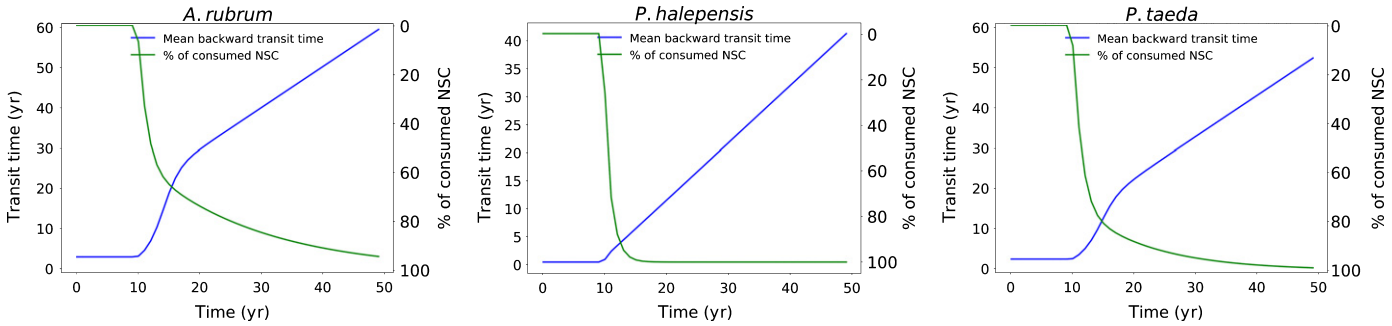

Fig. 6 Nonstructural carbon (NSC) mean backward transit time and the percentage of NSC consumption during 50 yr of the simulation for each species *Pinus halepensis*, *Acer rubrum* and *Pinus taeda*. The first 10 yr of the simulation represent the steady state, with trees growing under healthy conditions. After this, assimilation was set to zero to simulate carbon limitation for the subsequent 40 yr. For a given time step of the simulation there is a degree of consumption (green line) on the right axis, and there is a backward transit time (blue line) on the left axis. This mean backward transit time reflects the mean age of the carbohydrates being used in metabolism and growth in each time step of the simulations.

higher uncertainties than *P. taeda* and *P. halepensis* (Fig. S3). Some exceptionally high mean ages of the NSC could be obtained in very rare combinations of parameter values at the very limit of their distributions (Fig. S3).

Discussion

The whole-tree compartmental models for C allocation tested here allowed us to estimate: differences in the NSC age and transit time distributions that reflected C storage dynamics of different tree species; the change in the age of the NSC used under C limitation; and the main NSC cycling rates that influenced the NSC mean age and mean transit time in mature trees.

NSC dynamics between tree tissues and tree species

The predicted NSC age and transit time distributions indicated large differences between tree species that reflected differences in functional types – deciduous (*A. rubrum*) or evergreen (*P. taeda*) – and growth environments – highly limited (Mediterranean *P. halepensis*) and mesic growth conditions (temperate species) (Fig. 3). These differences reflected the locations where reserves accumulate, and how long they remain in each C pool. For instance, *A. rubrum* stored more old C, evidenced in the longer tail of the NSC age distribution, compared with *P. taeda* and *P. halepensis* (Fig. 3). The age distribution of NSC within each pool reflects the role of each NSC pool in C cycling and storage of mature trees. For temperate species, NSC was stored longer in the stem and coarse roots (SSNSC), with more old C present (Fig. 3). By contrast, *P. halepensis* did not show actual age differences between slow (stored NSC) and fast (active NSC) pools (Fig. 3), suggesting no capacity for long-term storage of NSC. However, it may also be possible that long-term storage pools were neglected by the assumptions made in this model (e.g. the fast and slow pools were associated with the sugar and starch compartments, respectively). These results demonstrate the difficulties of separating and measuring fast and slow cycling NSC pools, and highlight the utility of estimating NSC ages based on compartmental systems to identify and understand the C dynamics associated with these elusive C pools (Richardson *et al.*, 2015). Despite the fact that our mean NSC age estimates in leaf compartments were almost 1 year older than what has been reported previously (Keel *et al.*, 2007; Gaudinski *et al.*, 2009), our results predicted different C storage traits between tree species that range from slow C cycling trees that accumulate larger proportions of long-term reserves (e.g. *A. rubrum*) and fast C cycling trees with low accumulation of long-term reserves (e.g. *P. halepensis*).

Nonstructural C transit time distributions reflected the age composition of NSC reserves being used by trees in metabolism and growth. Our estimates showed that healthy trees used mainly young C (Fig. 5). The allocation of mainly young C to respiration and growth in mature healthy trees has been already documented (Carbone *et al.*, 2013; Muhr *et al.*, 2018). This behavior has been commonly explained by the 'last in, first out' hypothesis for using the NSC where the most recently fixed C entering the systems is the one that is used at first (Dietze *et al.*, 2014; Hartmann & Trumbore, 2016). In our models, this idea is partly represented by the differentiation between fast and slow NSC cycling pools in each tissue. This differentiation in organ NSC pools and compound NSC pools (fast and slow cycling pools) represents the spatial heterogeneity of the NSC ages within the tree. Partly in disagreement with the 'last in, first out' principle, previous studies have also shown that some old NSC is mixed in the metabolized CO_2 in healthy trees with nonlimiting assimilate supply, as a result of the continuous exchange of C between the active NSC and the stored NSC pools (Richardson *et al.*, 2012; Carbone *et al.*, 2013; Muhr *et al.*, 2013). This is in agreement with our results where the NSC transit time distributions (Fig. 5) showed that the C being used in metabolism and growth is a mixture of C of different ages. The transit time distribution is mainly determined by the age structure of the largest C source and the balance between C sources and sinks in the tree. In this sense, in healthy-mature trees, the inflow of new C greatly exceeds the retrieval of old stored C for sustaining metabolism and growth, which leads to the high abundance of young NSC in the trees and skewness of the distribution towards low values, with corresponding low values of mean transit time (Figs 3, 5). Therefore,

within our framework, healthy trees may use mainly young C as a result of its high abundance in the NSC pools, and its constant replenishment as a result of rapid assimilation of atmospheric C, and not because the younger C is more available as a result of its position in the tree. This concept is supported by the simulation results in Fig. 4 where the young C is depleted faster than the old C – owing to its relative high abundance – until eventually flattening the age distribution of the NSC in each pool.

In other words, our results provide a probabilistic interpretation for the use of young C for metabolism and growth. As young NSC is more abundant in storage pools, it has a greater probability of being used for plant function. These results provide a new perspective on the understanding of the NSC allocation to metabolism and growth, and also highlight the utility of obtaining the NSC transit time distribution in mature trees for understanding C source/sink imbalances.

Age structure of NSC reserves under C limitation

Under severe C limitation, the modeled trees used their NSC reserves to support metabolic needs and consequently the NSC mean transit time increased rapidly (Fig. 6). Previous studies that interrupted C assimilation by either girdling, harvesting of the main trunk, or hurricane damage also reported a rapid increase in the NSC mean transit time from very young C to C that is several years old. For instance, $^{14}CO_2$ respired from *Scleronema micranthum*, a measure of transit time, increased from 1 to 15 yr old over a year after girdling (Muhr *et al.*, 2018); stump resprouts in *A. rubrum* growing after trunk harvesting were found to be made of C up to 17 yr old (C e *et al.*, 2013); and up to 10-yr-old C was used to grow new roots for tropical trees after hurricane damage (Vargas *et al.*, 2009). In addition, D'Andrea *et al.,* (2019) reported that the mean age of sugars in the phloem of beech trees that were defoliated by frost late in spring increased to *c.* 5 yr within only a few weeks.

We were able to describe how this old C was used and for how long it could last by observing how the NSC mean transit time increased over time during our simulations. The NSC mean transit time increased in an exponential way that depended on the amount and the cycling speed of the reserves, followed by a linear phase that occurred when the NSC age distribution became flat and only described the aging of the remaining NSC (Fig. 6). We observed that the exponential increase in the NSC mean transit time described how the trees consume between 80% and 90% of the available C, depending on their storage strategy (Fig. 6). The NSC mean transit time towards the end of the exponential increase was higher (14–21 yr) than the reported age (12–17 yr) of the respired CO_2 of trees subjected to starvation (Carbone *et al.*, 2013; Muhr *et al.*, 2018). This difference can be explained by the fact that we did not represent mortality explicitly; therefore, the trees continued using reserves for a longer time than in experiments where the trees die before exhausting 80–90% of their reserves. Considering a consumption threshold between 50% and 60% (Mei *et al.*, 2015; Wiley *et al.*, 2019), the mean transit time is 5 and 10 yr for *P. taeda* and *A. rubrum*, respectively (Fig. 6), in agreement with what has been reported for starving trees. Our predictions also report a very slow consumption of the reserves when trees are under C limitation, taking between 2 and 5 yr to exhaust 80% of their reserves, and between 1 and 3 yr to reach the 50–60% of NSC consumption. Measurements in mature trees documented an up to three-fold faster increase in the NSC mean transit time than in our model (Carbone *et al.*, 2013; Muhr *et al.*, 2018). These discrepancies between our model estimates and NSC ages reported in empirical studies, along with the unexpected high mean NSC ages in leaves, could be a result of several factors:

- The parameters provided for our models may not fully represent the trees evaluated in the studies; more precise and exhaustive parameter estimation may be needed.
- The measurements may have been taken for trees that have not yet reached their steady state and therefore have higher transfer coefficients of C between pools.
- Additional fluxes and C compartments are not considered in the model, nor are other mechanisms such as trees' ability to control growth and respiration under stress, active NSC allocation to storage, or other nonlinearities in the model – thus, alternative model structures may be needed.
- Our source limitation simulations were restricted only to a complete cessation of C assimilation. Limiting conditions such as drought or severe physical damage, may also imply a limitation in the mobilization of the stored NSC or truncation of the NSC mass, which would reduce the quantity of stored NSC available and cause a quicker depletion of the NCS in the trees.
- Measurements of respired $^{14}CO_2$ in previous studies are restricted to the stem-wood and thus do not reflect the time that the increase in the mean NSC transit time would take for the whole tree.

Overall, this analysis allowed us to estimate the age composition of the NSC reserves being used at any point of the source limitation event and the time that each tree would take to exhaust those reserves.

Sensitivity of NSC mean age and mean transit time to changes in C allocation

Along with C source variability, sink strength also plays a fundamental role in NSC dynamics of mature trees. This is reflected in the NSC mean age and mean transit time if the assimilation of C is kept constant and numerical changes are induced in the cycling rates between C pools. The sensitivity analysis estimated that the efflux rate of C from the storage in the stem and the cycling rates of roots have a large influence on the NSC mean age and transit time, playing an important role in NSC dynamics (Fig. S1). But none of the C fluxes related to the foliage compartments had an important impact in the mean age and transit time of the trees' NSC (Fig. S1). Previous studies have shown that stored NSC in the stem and roots contributes to the respired CO_2 of trees under stress (Carbone *et al.*, 2006; Richardson *et al.*, 2012; Muhr *et al.*, 2013, 2018; Hartmann *et al.*, 2018), and that stored C below ground is vital to tree recovery after a disturbance (Schutz *et al.*, 2009; Hagedorn *et al.*, 2016; McDowell *et al.*, 2018). These allocation rates usually change when trees experience limiting

conditions (Nogués *et al.*, 2006; Wiley *et al.*, 2013, 2019; Hagedorn *et al.*, 2016), but the mechanism behind these changes remains uncertain (Chesney & Vasquez, 2007; Gaudinski *et al.*, 2009; Hartmann *et al.*, 2013; Mei *et al.*, 2015). When modeling C allocation as compartmental systems, we should be aware that changes in the fluxes between compartments can be a result of changes in the compartment mass (mass conservation principle) or changes in the cycling rates (transfer coefficients of the matrix ***B***) of the trees. In our simulations, the transfer coefficients remained constant, so changes in the fluxes after the C limitation only reflected changes in the mass of the compartments. However, a change in NSC dynamics occurs when the cycling rates change independently of the system C mass, which would change the C transfer coefficients between pools, as done in our sensitivity analysis. For instance, increasing the allocation rates from the storage in the wood to growth or respiration (Cs) would make the trees to cycle C faster, build younger reserves during their productive and healthy conditions, and increase the tree's vulnerability to starvation; while increasing the allocation of C to storage in the roots (Sr) would make them slower cyclers, build older reserves and be more resilient to low productivity periods (Fig. S2). Based on our models, we have estimated how cycling rates drive the NSC age and transit time distributions of mature trees.

Limitations and conclusions

Comparisons between the estimated NSC mean age and mean transit time with empirical measurements can serve as important diagnostics for model evaluation (Ceballos-Núñez *et al.*, 2018). However, the models used here are not easy to parameterize and require a large number of observations. Our model parameters are rough estimates of the fluxes for an average healthy mature tree of each species (ACGCA model) or population of trees (*P. halepensis* case), and their structure may misrepresent other mechanisms. They are also constrained by the assumptions made when the parameters were estimated; for example, the NSC allocation to storage happens passively when C supply exceeds demand. These parameter estimates can be improved with empirical research, theoretical studies, and statistical approaches that consider variability within and among trees as well as alternative assumptions regarding NSC allocation. Furthermore, our representations are very simple and do not consider nonlinear interactions and other important fluxes, such as the exchange of C with the rhizosphere (Epron *et al.*, 2011), allocation of C to reproduction (Hacket-Pain *et al.*, 2018), emissions of biogenic volatile organic compounds (BVOC) (Epron *et al.*, 2012), and allocation to defense compounds (Huang *et al.*, 2019a), which also play an important role for determining NSC dynamics. However, information about these fluxes is still scarce and uncertain. Nevertheless, our results open the possibility to better understand NSC dynamics in mature trees based on estimated NSC ages and transit times in different tree organs of species with contrasting life strategies and growth environments. Our estimates are relevant for characterizing general differences in the NSC dynamics in contrasting tree species, identifying different storage traits based on plant type and growth environment; predicting how trees use their reserves under stress (e.g. the exponential-linear increase of the NSC transit time as trees exhaust their reserves); providing a plausible probabilistic interpretation about why trees consume primarily young C during healthy stages and why this shifts after a prolonged C limitation; and identifying the determinant sink fluxes in NSC dynamics for mature trees.

Acknowledgements

We want to thank Markus Müller for important support in writing the code for running the models and simulations. This work was supported by the German Israeli Fund grant number I-1334-307.8, the German Research Foundation through its Emmy Noether Program (SI 1953/2–1), and the German Centre for Integrative Biodiversity Research (iDiv) Halle-Jena-Leipzig, D-04103 Leipzig.

Author contributions

CAS and DH-R conceived the idea. DH-R, JM, HH, CR, ST and CAS contributed to the design of the work. DH-R performed the computations and wrote the manuscript. DH-R, JM, HH, CR, ST and CAS revised the manuscript and gave important and critical input.

ORCID

Henrik Hartmann https://orcid.org/0000-0002-9926-5484
David Herrera-Ramírez https://orcid.org/0000-0001-6183-8032
Jan Muhr https://orcid.org/0000-0001-5264-0243
Christine Römermann https://orcid.org/0000-0003-3471-0951
Carlos A. Sierra https://orcid.org/0000-0003-0009-4169
Susan Trumbore https://orcid.org/0000-0003-3885-6202

References

Anderegg WRL, Anderegg LDL. 2013. Hydraulic and carbohydrate changes in experimental drought-induced mortality of saplings in two conifer species. *Tree Physiology* **33**: 252–260.

Bolin B, Rodhe H. 1973. A note on the concepts of age distribution and transit time in natural reservoirs. *Tellus* **25**: 58–62.

Bréda N, Huc R, Granier A, Dreyer E. 2006. Temperate forest trees and stands under severe drought: a review of ecophysiological responses, adaptation processes and long-term consequences. *Annals of Forest Science* **63**: 625–644.

Campolongo F, Cariboni J, Saltelli A. 2007. An effective screening design for sensitivity analysis of large models. *Environmental Modelling & Software* **22**: 1509–1518.

Carbone MS, Czimczik CI, Keenan TF, Murakami PF, Pederson N, Schaberg PG, Xu X, Richardson AD. 2013. Age, allocation and availability of nonstructural carbon in mature red maple trees. *New Phytologist* **200**: 1145–1155.

Carbone MS, Czimczik CI, Mcduffee KE, Trumbore SE. 2006. Allocation and residence time of photosynthetic products in a boreal forest using a low-level 14C pulse-chase labeling technique. *Global Change Biology* **13**: 466–477.

Carnicer J, Coll M, Ninyerola M, Pons X, Sanchez G, Penuelas J. 2011. Widespread crown condition decline, food web disruption, and amplified tree

mortality with increased climate change-type drought. *Proceedings of the National Academy of Sciences, USA* **108**: 1474–1478.

Ceballos-Núñez V, Richardson AD, Sierra CA. 2018. Ages and transit times as important diagnostics of model performance for predicting carbon dynamics in terrestrial vegetation models. *Biogeosciences* **15**: 1607–1625.

Chesney P, Vasquez N. 2007. Dynamics of non-structural carbohydrate reserves in pruned *Erythrina poeppigiana* and *Gliricidia sepium* trees. *Agroforestry Systems* **69**: 89–105.

Cuntz M, Mai J, Zink M, Thober S, Kumar R, Schäfer D, Schrön M, Craven J, Rakovec O, Spieler D *et al.* 2015. Computationally inexpensive identification of noninformative model parameters by sequential screening. *Water Resources Research* **51**: 6417–6441.

D'Andrea E, Rezaie N, Battistelli A, Gavrichkova O, Kuhlmann I, Matteucci G, Moscatello S, Proietti S, Scartazza A, Trumbore S *et al.* 2019. Winter's bite: beech trees survive complete defoliation due to spring late-frost damage by mobilizing old C reserves. *New Phytologist* **224**: 625–631.

Dietze MC, Sala A, Carbone MS, Czimczik CI, Mantooth JA, Richardson AD, Vargas R. 2014. Nonstructural Carbon in Woody Plants. *Annual Review of Plant Biology* **65**: 667–687.

Epron D, Bahn M, Derrien D, Lattanzi FA, Pumpanen J, Gessler A, Högberg P, Maillard P, Dannoura M, Gérant D *et al.* 2012. Pulse-labelling trees to study carbon allocation dynamics: a review of methods, current knowledge and future prospects. *Tree Physiology* **32**: 776–798.

Epron D, Ngao J, Dannoura M, Bakker MR, Zeller B, Bazot S, Bosc A, Plain C, Lata JC, Priault P *et al.* 2011. Seasonal variations of belowground carbon transfer assessed by *in situ* $^{13}CO_2$ pulse labelling of trees. *Biogeosciences* **8**: 1153–1168.

Gaudinski JB, Torn MS, Riley WJ, Swanston C, Trumbore SE, Joslin JD, Majdi H, Dawson TE, Hanson PJ. 2009. Use of stored carbon reserves in growth of temperate tree roots and leaf buds: analyses using radiocarbon measurements and modeling. *Global Change Biology* **15**: 992–1014.

Hacket-Pain AJ, Ascoli D, Vacchiano G, Biondi F, Cavin L, Conedera M, Drobyshev I, Liñán ID, Friend AD, Grabner M *et al.* 2018. Climatically controlled reproduction drives interannual growth variability in a temperate tree species. *Ecology Letters* **21**: 1833–1844.

Hagedorn F, Joseph J, Peter M, Luster J, Pritsch K, Geppert U, Kerner R, Molinier V, Egli S, Schaub M *et al.* 2016. Recovery of trees from drought depends on belowground sink control. *Nature Plants* **2**: 16111.

Hartmann H, Adams HD, Hammond WM, Hoch G, Landhäusser SM, Wiley E, Zaehle S. 2018. Identifying differences in carbohydrate dynamics of seedlings and mature trees to improve carbon allocation in models for trees and forests. *Environmental and Experimental Botany* **152**: 7–18.

Hartmann H, Trumbore S. 2016. Understanding the roles of nonstructural carbohydrates in forest trees – from what we can measure to what we want to know. *New Phytologist* **211**: 386–403.

Hartmann H, Ziegler W, Trumbore S. 2013. Lethal drought leads to reduction in nonstructural carbohydrates in Norway spruce tree roots but not in the canopy. *Functional Ecology* **27**: 413–427.

Huang J, Forkelová L, Unsicker SB, Forkel M, Griffith DWT, Trumbore S, Hartmann H. 2019a. Isotope labeling reveals contribution of newly fixed carbon to carbon storage and monoterpenes production under water deficit and carbon limitation. *Environmental and Experimental Botany* **162**: 333–344.

Huang J, Hammerbacher A, Weinhold A, Reichelt M, Gleixner G, Behrendt T, Dam NM, Sala A, Gershenzon J, Trumbore S *et al.* 2019b. Eyes on the future – evidence for trade-offs between growth, storage and defense in Norway spruce. *New Phytologist* **222**: 144–158.

Iooss B, Janon A, Pujol G, Broto B, Boumhaout K, Da Veiga S, Delage T, Fruth J, Gilquin L, Guillaume J *et al.* 2019. *Sensitivity: global sensitivity analysis of model outputs.* [WWW document] URL https://cran.r-project.org/web/packages/sensitivity/index.html.

IPCC. 2018. Summary for policymakers. In: Waterfield T, Masson-Delmotte V, Zhai P, Pörtner HO, Roberts D, Skea J, Shukla PR, Pirani A, Moufouma-Okia W, Péan C *et al.* eds. *Global warming of 1.5°C. An IPCC Special Report on the impacts of global warming of 1.5°C above pre-industrial levels and related global greenhouse gas emission pathways, in the context of strengthening the global response to the threat of climate change, sustainable development, and efforts to eradicate poverty.* Geneva, Switzerland: World Meteorological Organization.

Jacquez JA, Simon CP. 1993. Qualitative theory of compartmental systems. *SIAM Review* **35**: 43–79.

Keel SG, Siegwolf RTW, Jäggi M, Körner C. 2007. Rapid mixing between old and new C pools in the canopy of mature forest trees. *Plant, Cell & Environment* **30**: 963–972.

Klein T, Hartmann H. 2018. Climate change drives tree mortality (J Sills, Ed.). *Science* **362**: 758.

Klein T, Hoch G. 2015. Tree carbon allocation dynamics determined using a carbon mass balance approach. *New Phytologist* **205**: 147–159.

Lacointe A, Deleens E, Ameglio T, Saint-Joanis B, Lelarge C, Vandame M, Song GC, Daudet FA. 2004. Testing the branch autonomy theory: a $^{13}C/^{14}C$ double-labelling experiment on differentially shaded branches. *Plant, Cell & Environment* **27**: 1159–1168.

Martínez-Vilalta J, Sala A, Asensio D, Galiano L, Hoch G, Palacio S, Piper FI, Lloret F. 2016. Dynamics of non-structural carbohydrates in terrestrial plants: a global synthesis. *Ecological Monographs* **86**: 495–516.

McDowell N, Allen CD, Anderson-Teixeira K, Brando P, Brienen R, Chambers J, Christoffersen B, Davies S, Doughty C, Duque A *et al.* 2018. Drivers and mechanisms of tree mortality in moist tropical forests. *New Phytologist* **219**: 851–869.

Mei L, Xiong Y, Gu J, Wang Z, Guo D. 2015. Whole-tree dynamics of non-structural carbohydrate and nitrogen pools across different seasons and in response to girdling in two temperate trees. *Oecologia* **177**: 333–344.

Metzler H, Müller M, Sierra CA. 2018. Transit-time and age distributions for nonlinear time-dependent compartmental systems. *Proceedings of the National Academy of Sciences, USA* **115**: 1150–1155.

Metzler H, Sierra CA. 2018. Linear autonomous compartmental models as continuous-time markov chains: transit-time and age distributions. *Mathematical Geosciences* **50**: 1–34.

Morris MD. 1991. Factorial sampling plans for preliminary computational experiments. *Technometrics* **33**: 161–174.

Muhr J, Angert A, Negrón-Juárez RI, Muñoz WA, Kraemer G, Chambers JQ, Trumbore SE. 2013. Carbon dioxide emitted from live stems of tropical trees is several years old. *Tree Physiology* **33**: 743–752.

Muhr J, Messier C, Delagrange S, Trumbore S, Xu X, Hartmann H. 2016. How fresh is maple syrup? Sugar maple trees mobilize carbon stored several years previously during early springtime sap-ascent. *New Phytologist* **209**: 1410–1416.

Muhr J, Trumbore S, Higuchi N, Kunert N. 2018. Living on borrowed time – Amazonian trees use decade-old storage carbon to survive for months after complete stem girdling. *New Phytologist* **220**: 111–120.

Nogués S, Damesin C, Tcherkez G, Maunoury F, Cornic G, Ghashghaie J. 2006. $^{13}C/^{12}C$ isotope labelling to study leaf carbon respiration and allocation in twigs of field-grown beech trees. *Rapid Communications in Mass Spectrometry* **20**: 219–226.

Nunez S, Arets E, Alkemade R, Verwer C, Leemans R. 2019. Assessing the impacts of climate change on biodiversity: is below 2°C enough? *Climatic Change* **154**: 351–365.

Ogle K, Pacala SW. 2009. A modeling framework for inferring tree growth and allocation from physiological, morphological and allometric traits. *Tree Physiology* **29**: 587–605.

Oliveira AS, Rajão RG, Soares Filho BS, Oliveira U, Santos LRS, Assunção AC, Hoff R, Rodrigues HO, Ribeiro SMC, Merry F *et al.* 2019. Economic losses to sustainable timber production by fire in the Brazilian Amazon. *The Geographical Journal* **185**: 55–67.

Overdieck D. 2016. Nonstructural and structural carbohydrates. *CO_2, temperature, and trees: experimental approaches.* Singapore: Springer Singapore, 65–79.

Parkinson S, Young P. 1998. Uncertainty and sensitivity in global carbon cycle modelling. *Climate Research* **9**: 157–174.

Pugh TAM, Lindeskog M, Smith B, Poulter B, Arneth A, Haverd V, Calle L. 2019. Role of forest regrowth in global carbon sink dynamics. *Proceedings of the National Academy of Sciences, USA* **116**: 4382.

Richardson AD, Carbone MS, Huggett BA, Furze ME, Czimczik CI, Walker JC, Xu X, Schaberg PG, Murakami P. 2015. Distribution and mixing of old and new nonstructural carbon in two temperate trees. *New Phytologist* **206**: 590–597.

Richardson AD, Carbone MS, Keenan TF, Czimczik CI, Hollinger DY, Murakami P, Schaberg PG, Xu X. 2012. Seasonal dynamics and age of

stemwood nonstructural carbohydrates in temperate forest trees. *New Phytologist* **197**: 850–861.

Schutz AEN, Bond WJ, Cramer MD. 2009. Juggling carbon: allocation patterns of a dominant tree in a fire-prone savanna. *Oecologia* **160**: 235–246.

Sierra CA, Müller M, Trumbore SE. 2014. Modeling radiocarbon dynamics in soils: SoilR version 1.1. *Geoscientific Model Development* **7**: 1919–1931.

Strand J. 2017. Modeling the marginal value of rainforest losses: a dynamic value function approach. *Ecological Economics* **131**: 322–329.

Trugman AT, Detto M, Bartlett MK, Medvigy D, Anderegg WRL, Schwalm C, Schaffer B, Pacala SW. 2018. Tree carbon allocation explains forest drought-kill and recovery patterns. *Ecology Letters* **21**: 1552–1560.

Trumbore S, Czimczik CI, Sierra CA, Muhr J, Xu X. 2015. Non-structural carbon dynamics and allocation relate to growth rate and leaf habit in California oaks. *Tree Physiology* **35**: 1206–1222.

Vargas R, Trumbore SE, Allen MF. 2009. Evidence of old carbon used to grow new fine roots in a tropical forest. *New Phytologist* **182**: 710–718.

von Arx G, Arzac A, Fonti P, Frank D, Zweifel R, Rigling A, Galiano L, Gessler A, Olano JM. 2017. Responses of sapwood ray parenchyma and non-structural carbohydrates of *Pinus sylvestris* to drought and long-term irrigation. *Functional Ecology* **31**: 1371–1382.

Wiley E, Huepenbecker S, Casper BB, Helliker BR. 2013. The effects of defoliation on carbon allocation: can carbon limitation reduce growth in favour of storage? *Tree Physiology* **33**: 1216–1228.

Wiley E, King CM, Landhäusser SM. 2019. Identifying the relevant carbohydrate storage pools available for remobilization in aspen roots (D Tissue, Ed.). *Tree Physiology* **39**: 1109–1120.

Supporting Information

Additional Supporting Information may be found online in the Supporting Information section at the end of the article.

Fig. S1. Mean sensitivity value μ and its correspondent variance σ for each flux of each species – *Pinus halepensis*, *Acer rubrum* and *Pinus taeda* – calculated by the elementary effects method.

Fig. S2. Association between the most sensitive NSC transfer coefficients (Fig. S1) and the mean age and mean transit time for each species: *Pinus halepensis*, *Acer rubrum* and *Pinus taeda*.

Fig. S3. Uncertainties associated with the model parameters with the largest influence in the NSC mean age and mean transit time per species *Pinus halepensis*, *Acer rubrum* and *Pinus taeda*.

Please note: Wiley Blackwell are not responsible for the content or functionality of any Supporting Information supplied by the authors. Any queries (other than missing material) should be directed to the *New Phytologist* Central Office.